Jpn. J. Appl. Phys. Vol. 38 (1999) pp. 2983–2987
Part 1, No. 5A, May 1999

Direct Measurements of Femtosecond Energy Dissipation Processes of Hot Electrons in a Gold Film

Akihide HIBARA, Tomohiro MORISHITA, Isao TSUYUMOTO, Akira HARATA[1],
Takehiko KITAMORI and Tsuguo SAWADA*

Department of Applied Chemistry, School of Engineering, The University of Tokyo, 7-3-1 Hongo, Bunkyo-ku, Tokyo 113-8656, Japan
[1]*Department of Molecular Science and Technology, Graduate School of Engineering Science, Kyushu University, 6-1 Kasugakoen, Kasuga, Fukuoka 816-8580, Japan*

(Received November 16, 1998; accepted for publication February 23, 1999)

Energy dissipation processes of hot electrons in a gold thin film were measured by a femtosecond time-resolved transient reflecting grating method. The processes were analyzed using the two-temperature model and the theory of the transient grating method. It was found that the electron-phonon coupling and thermal diffusion processes could be investigated independently. Temperature dependence of the electron-phonon coupling factor and the thermal conductivity was investigated quantitatively. The results suggested that the nonthermal states of hot electrons still contribute to the dissipation processes on time scales of several picoseconds.

KEYWORDS: hot electrons, transient reflecting grating method, electron-phonon coupling, transport phenomena

1. Introduction

The ultrafast dynamics of photoexcited electrons in metals have been intensely investigated, using fs-laser techniques, in order to study nonequilibrium systems and particle-like behavior of electrons in solids.[1)] The thermalization processes of the photoexcited electrons were directly measured by a two-photon photoemission method, and ultrafast electron dynamics on metal surfaces was discussed.[2,3)] These processes have also been measured by a transient reflecting (TR) method. The TR method measures reflectivity changes (ΔR) by electron temperature rise (ΔT_e) after the thermalization. The TR measurements showed that the photoexcited electrons before thermalization have ballistic characteristics[4,5)] and are thermalized within several hundred femtoseconds in gold films.[6)] Energy dissipation processes of hot electrons after the thermalization have been analyzed by the two-temperature model (TTM), based on thermal diffusion and electron-phonon coupling.[7–9)] Intense interest has been shown toward these two processes, not only in fundamental physics, but also in short-pulse laser-applications, such as material processing. However, quantitative treatment has been difficult, especially for the thermal conductivity κ and the electron-phonon coupling factor G. When the pump pulse is focused on the metal surface and the T_e gradient is induced in a spot size of several μm scale, the energy dissipation rate of hot electrons by thermal diffusion ($1/\tau_D$) becomes comparable to that by electron-phonon coupling ($1/\tau_{e\text{-}p}$). To quantify and separate these rates, it has been necessary to control the initial T_e gradient and to measure the energy dissipation processes directly.

The transient reflecting grating (TRG) method is suitable for investigating the energy dissipation process of hot electrons. In the TRG method, sample surfaces are excited, with periodic patterns induced by interference between two pump pulses crossing on a sample surface. The periodic patterns can be controlled by changing the optical setup (see §2). The fundamental properties of the TRG method, such as diffraction efficiency and surface selectivity have been well investigated.[10)] In addition, the usefulness of the TRG method has been demonstrated in many applications, such as elucidation carrier dynamics in semiconductors.[11,12)] The thermal and acoustic properties of metal surfaces have been investigated by ps-TRG measurements.[13,14)] Recently, the TRG method under surface plasmon resonance conditions has also been developed.[15)] In fs-time-resolved measurements of metal surfaces, the TRG method is expected to be useful, especially in quantitative treatment of hot electron transport and electron-phonon coupling in the surface plane.

Here, we report direct measurements of the energy dissipation processes of hot electrons in a gold film of 100 nm thickness using the fs-TRG method. The gold film was excited by high laser fluence ($\sim$ mJ·cm^{-2}) and high photon energy ($\lambda_{pump} = 400$ nm). Since the thermalization process can be regarded as instantaneous on highly excited surfaces,[16)] the hot electrons with electron temperature T_e were dynamically investigated in our fs-TRG measurements. The energy dissipation dynamics of the hot electrons was analyzed by TTM and the theory of the transient grating method.[17)]

2. Experimental

A schematic figure of the TRG method is shown in Fig. 1. Methodological descriptions for the TRG technique have been presented in refs. 10 and 17, so only a summary is given here. TRG responses are measured by a pump-probe technique. Two pump pulses of the same wavelength λ_{pump} cross on a metal surface and form an optical interference pattern with the fringe spacing Λ which is tunable by changing the crossing angle of the two pump pulses 2θ, as $\Lambda = \lambda_{pump}/(2\sin\theta)$. Thus, the interference pattern along the x-direction excited by p-polarized beams can be written as $2I + I\cos(2\pi x/\Lambda)$, where I is the one-side intensity of the pump pulse. The temporally generated interference fringes act as a transient diffraction grating. A probe pulse ($\lambda_{probe} = 800$ nm) is incident normal to the grating, after passing through an optical delay line, and is diffracted by the grating. Intensities of the diffracted light are recorded as TRG signals.

TRG experiments were performed using a regeneratively amplified Ti:sapphire laser system which had an autocorrelation of 200 fs, a wavelength of 800 nm and a repetition rate of 1 kHz. The pump light was frequency-doubled and split in two parts. Each pump pulse had a spot size of 600 μm, a

*To whom correspondence should be addressed. E-mail address:t sawada@hongo.ecc.u-tokyo.ac.jp

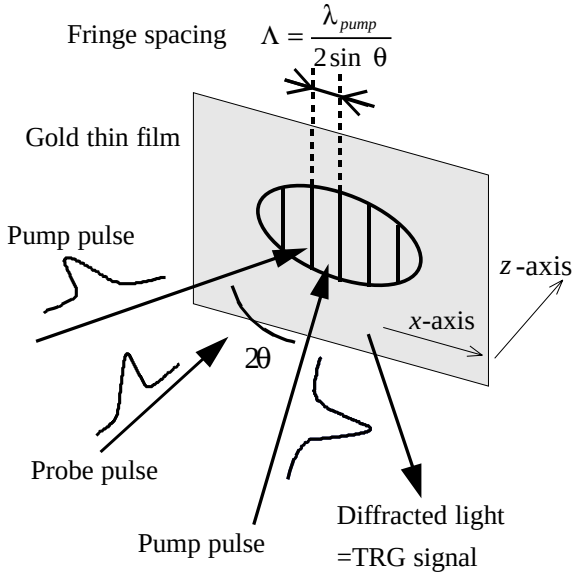

Fig. 1. A schematic figure of the TRG method.

fluence I of 0.38 to 2.25 mJ·cm^{-2}, and p-polarization. Initial electron temperatures (T_{e0}) were estimated as 1700 to 4200 K from the absorbed energy and electronic heat capacity in the detection volume. The fringe spacings were set to 1.1, 1.5, 2.1 and 2.5 μm by controlling the crossing angles. The polarizations of pump and probe beams were perpendicular to each other. The diffracted light was detected by a positive-intrinsic-negative (PIN) photodiode. The output of the photodiode was fed into a fast-gated-integrator and its average signal was recorded as a TRG response. A polycrystalline gold thin film deposited on a glass plate was used for the measurements. The reflectivity R of the gold film was measured as 0.4 at $\lambda_{pump} = 400$ nm. The penetration depths of the pump beam ($\lambda_{pump} = 400$ nm) and the probe beam ($\lambda_{probe} = 800$ nm) were calculated as 16 and 12 nm, respectively. All the experiments were performed in air at 296 K.

3. Theory

To analyze the energy dissipation processes, we used the two-temperature model (TTM).[7] The TTM assumes that the electron and lattice systems are in local equilibrium, that the electron temperature T_e is not in equilibrium with the lattice temperature T_l on a time scale of several picoseconds, and that T_e is coupled with T_l by electron-phonon coupling. The evolution of the systems can be written as a set of coupled differential equations. Namely,

$$\gamma T_e \frac{\partial T_e}{\partial t} = \nabla(\kappa \nabla T_e) - G(T_e - T_l) + Q, \tag{1a}$$

$$C_l \frac{\partial T_l}{\partial t} = G(T_e - T_l), \tag{1b}$$

where γT_e and C_l are the electronic and lattice heat capacities, G is the electron-phonon coupling factor, κ is the thermal conductivity, and Q is the energy source term. In eq. (1b), diffusion and energy source terms are neglected on the basis of physical considerations. Here, we assume that the electron temperature decay is approximately equal to the temporal evolution of $T_e - T_l$ and it is expressed by an exponential function. Under these assumptions, the decay time of the electron temperature τ_e can be derived from eqs. (1a) and (1b).

$$\begin{aligned}\frac{1}{\tau_e} &= -\frac{\partial}{\partial t}[\ln(T_e - T_l)] \\ &= \frac{1}{\tau_{e\text{-}p}} + \frac{1}{\tau_D}\end{aligned} \tag{2}$$

Here $\tau_{e\text{-}p}$ and τ_D are decay times by electron-phonon coupling and thermal diffusion, respectively, and are written as

$$\frac{1}{\tau_{e\text{-}p}} = \frac{G}{\gamma T_e} + \frac{G}{C_l}, \tag{2a}$$

$$\frac{1}{\tau_D} = \frac{\nabla(\kappa \nabla T_e)}{\gamma T_e (T_e - T_l)}. \tag{2b}$$

From eqs. (2), (2a) and (2b), the decay time τ_e can be estimated by averaging eqs. (2a) and (2b) temporally and spatially. To our knowledge, there have been no reports on the estimation hot electron energy loss rate including the diffusion term. In most conventional investigations by TR measurements,[6] eq. (2b) has been neglected. This approximation is valid only when film thickness is comparable to light penetration depth and the spot size of the pump beam is sufficiently large to neglect diffusion in the surface plane.

To clarify the thermal diffusion of hot electrons, the diffusion term was divided into two parts; thermal diffusion in the direction of the excitation fringe (parallel to the surface, x-axis in Fig. 1) and that in the thickness direction (perpendicular to the surface, z-axis in Fig. 1). The contributions of these two diffusion parts to TRG responses are very different. Under our experimental setup of excitation fringe spacings (1.1 to 2.5 μm) and the 100-nm-thick gold target, decay rates for the diffusion part parallel to the surface plane are estimated to be nearly comparable to the rates of electron-phonon coupling. In contrast, decay rates for the diffusion part perpendicular to the surface are much faster because of its higher temperature gradient.

The calculated temperature distributions along x- and z-directions are shown in Figs. 2(a) and 2(b), respectively. The full scale of the transverse axis of Fig. 2(a) corresponds to one period of the excitation fringe. The distributions are numerically calculated by eqs. (1a) and (1b) under the excitation conditions of $Q = 2.25$ mJ·cm^{-1}, $\Lambda = 1.1\,\mu$m and the pulse width of 200 fs using the values of γ, C_l, G and κ for Au[18,19] ($\gamma = 67.6$ J·m^{-3}·K^{-2}, $C_l = 2.5 \times 10^6$ J·m^{-3}·K^{-1}, $G = 3.5 \times 10^{16}$ W·m^{-3}·K^{-1} and $\kappa = 317$ W·m^{-1}·K^{-1}). As shown in Figs. 2(a) and 2(b), the temperature distribution along the z-axis becomes nearly homogeneous on a time scale of 1 ps while that along the x-axis is still clearly inhomogeneous at the delay time of 2 ps. This means that the diffusion occurring perpendicular to the surface is very quickly and has little effect on the TRG responses. Therefore, the diffusion term (eq. (2b)) may be regarded as one-dimensional in the direction of the excitation fringe (x-axis). Under this condition, eq. (2) can be transformed by using the theory of the transient grating method:[17]

$$\frac{1}{\tau_e} = \frac{1}{\tau_{e\text{-}p}} + D\left(\frac{2\pi}{\Lambda}\right)^2, \tag{3}$$

where D is the thermal diffusivity of the hot electrons. Equation (3) means that $\tau_{e\text{-}p}$ and D can be calculated from the relationship between τ_e and Λ. To obtain thermal conductivities κ and electron-phonon coupling factors G from eqs. (2) and (3), a characteristic electron-temperature should be defined. The

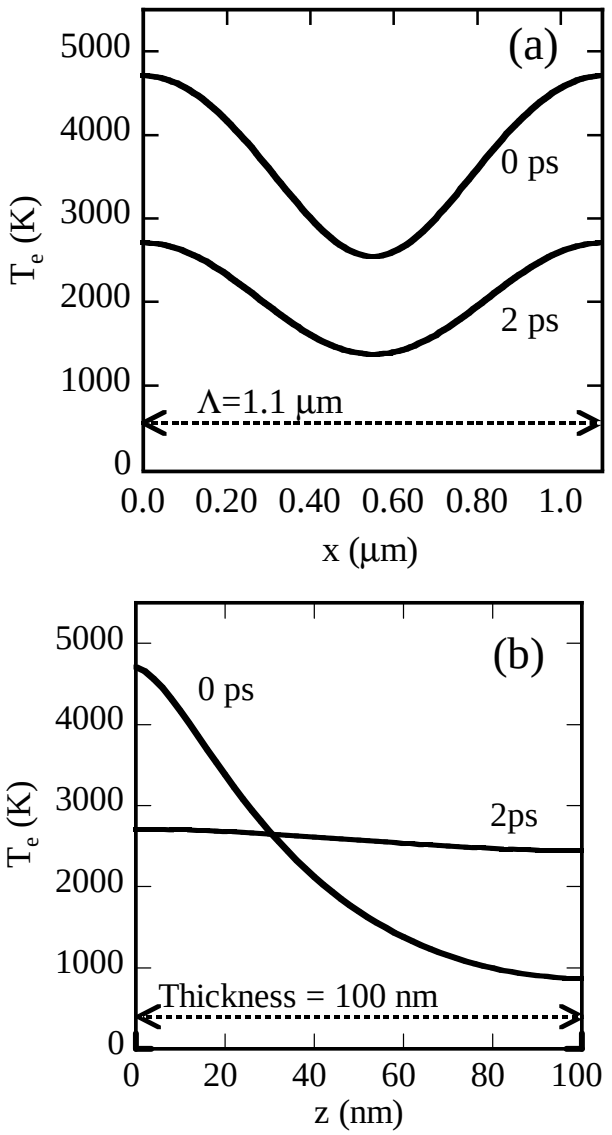

Fig. 2. (a)Temperature distributions for delay times of 0 and 2 ps in the direction of the excitation fringe at the surface. (b) Temperature distributions in the thickness direction at $x = 0$ in (a). The distributions are calculated numerically by eqs. (1a) and (1b).

mean initial electron-temperature in the probe volume T_{e0} was chosen as the characteristic temperature.[6,16)]

4. Results and Discussion

Typical TRG responses with a fringe spacing Λ of 1.1 μm and pump fluence I of 0.75 and 2.25 mJ·cm^{-2} are shown in Fig. 3. The decay curves in Fig. 3 denote only electronic energy dissipation processes because the generation of longitudinal and surface acoustic waves observed in ps-TRG measurements[13)] should occur on a time scale of several tens of picoseconds. The solid lines in Fig. 3 are best-fit results of an exponential function. The exponential function corresponds to the decay of the intensity of the diffracted light, which is proportional to $(\Delta\epsilon)^2$.[17)] For an ambient temperature of ~300 K, $\Delta\epsilon$ is related to the electron temperature rise as $\Delta\epsilon \propto \Delta T_e$. Therefore, the decay time of the fitted exponential function corresponds to half the decay time of electron temperature τ_e. As shown in Fig. 3, τ_e depends strongly on pump fluence I.

Dependence of the decay times τ_e on pump fluence I for

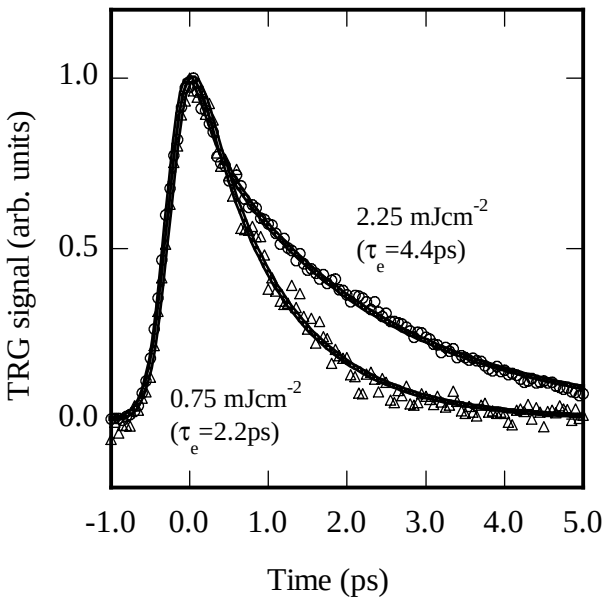

Fig. 3. TRG responses on a 100-nm-thick gold film with pump fluence of 0.75 and 2.25 mJ·cm^{-2} and an excitation fringe spacing of 1.1 μm. Solid lines: best-fit results by an exponential function which convoluted the temporal shape of the pump and probe pulses.

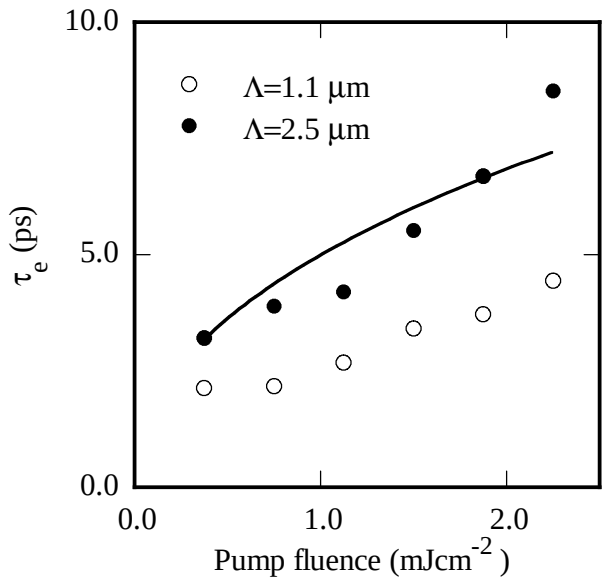

Fig. 4. Dependence of the decay times of electron temperature τ_e on pump fluences for Λ of 1.1 and 2.5 μm. Solid line: theoretical values given by eq. (2a).

Λ of 1.1 and 2.5 μm is shown in Fig. 4. The solid line shows the theoretical values of $\tau_{e\text{-}p}$ estimated by eq. (2a). The decay times for $\Lambda = 1.1\,\mu$m are clearly shorter than those for $\Lambda = 2.5\,\mu$m. This means that the diffusion term in eq. (2) affects τ_e. To obtain the thermal diffusivity D in eq. (3), the dependence of the decay times τ_e on the excitation fringe spacings Λ is shown in Fig. 5. The solid lines in Fig. 5 are the least-squares-fitted data of eq. (3). Obtained values of D and $\tau_{e\text{-}p}$ for various pump fluences I are summarized in Table I. Initial electron temperatures T_{e0} are calculated from deposited energies and temperature-dependent heat capacities. Since two time-coincident pump pulses were crossed on the sample surface in the TRG measurements, $2I \times (1 - R)$ was

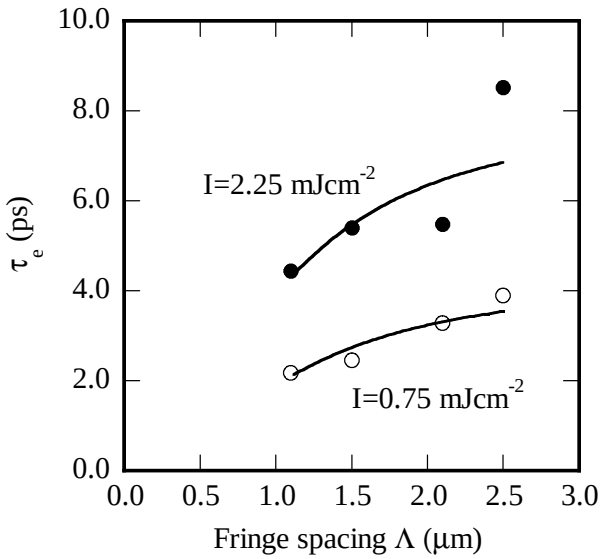

Fig. 5. Dependence of the decay times τ_e on the excitation fringe spacings Λ. Solid lines: least-squares-fitted data of eq. (3).

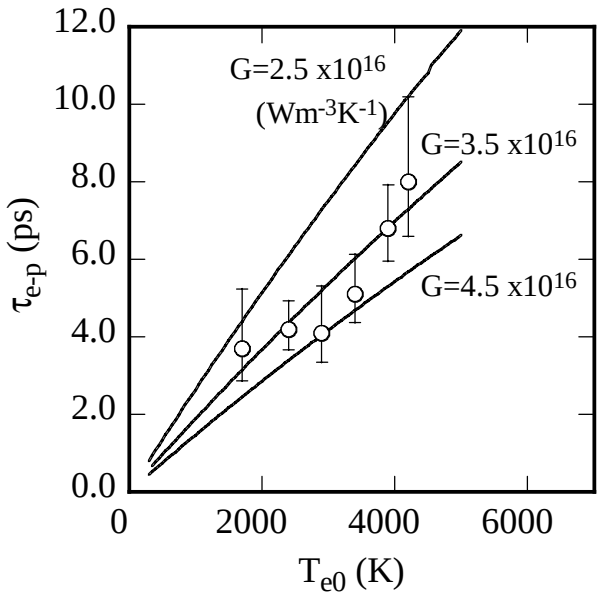

Fig. 6. Dependence of the decay times $\tau_{e\text{-}p}$ on the initial electron temperature T_{e0}. Solid lines: theoretical values calculated by eq. (2a) for $G = 2.5 \times 10^{16}$, 3.5×10^{16}, $4.5 \times 10^{16}\,\mathrm{W{\cdot}m^{-3}{\cdot}K^{-1}}$.

Table I. Obtained values of D and $\tau_{e\text{-}p}$ for various pump fluences I. Initial electron temperatures T_{e0} are calculated from deposited energies and heat capacities of the detection volume.

I (mJ·cm^{-2})	D (10^3 m^2·s^{-1})	$\tau_{e\text{-}p}$ (ps)	T_{e0} (K)
0.38	7.2	3.7	1700
0.75	7.4	4.2	2400
1.13	4.9	4.1	2900
1.50	3.3	5.1	3400
1.88	4.0	6.8	3900
2.25	3.2	8.0	4200

chosen as the spatially averaged deposited energy. This simple assumption was justified by comparison of the estimated T_{e0} and the numerically calculated one.

Our TRG measurements demonstrated that the electron-phonon coupling process could be distinguished from the thermal diffusion on the metal surfaces, as shown in Table I. This means that the electron-phonon coupling process and thermal diffusion can be investigated independently and quantitatively.

First, we discuss the electron-phonon coupling process. Dependence of the decay times $\tau_{e\text{-}p}$ on the initial electron temperature T_{e0} is shown in Fig. 6. The error bars in the plot indicate the standard deviations of the fitted values. The theoretical values calculated by eq. (2a) are also shown in Fig. 6 (solid lines) by using three temperature-independent electron-phonon coupling factors. The values calculated with $G = 3.5 \times 10^{16}\,\mathrm{W{\cdot}m^{-3}{\cdot}K^{-1}}$, which was previously reported,[19,20] seem to agree with the experimental ones. However, our results seem to include the systematic errors relative to the theoretical values. This may correspond to the temperature dependence of the electron-phonon coupling. Although the temperature dependence of G has been investigated experimentally and theoretically by many investigators,[21,22] the exact dependence has not been clarified. The temperature dependence has been expressed by $G \propto T_e^n$ with $1 < n < 3$ in one previous report[21] and $0.5 < n < 1$ in another report.[22] When these findings are considered, the relationship between T_e and $\tau_{e\text{-}p}$ (eq. (2a)) is expressed by $\tau_{e\text{-}p} \propto T_e^m$ with $m < 1$. However, our results appear to show the relationship $\tau_{e\text{-}p} \propto T_e^m$ with $m > 1$, which corresponds to $G \propto T_e^n$ with $n < 0$. This suggests that the coupling strength between the electron and phonon systems becomes weak in the high T_e region. In addition, nonthermal states, which have been reported to exist before thermalization processes,[4] are suggested to affect the energy dissipation processes even on time scales of picoseconds. While nonthermal behaviors of the hot electrons within a picosecond have been reported by several groups,[2,4,5] those on a longer time scale have not, to our knowkedge, been reported. Nonthermal processes on time scales of picoseconds are suggested in this paper.

Next, the thermal diffusion process is discussed. The thermal conductivities κ can be calculated with the thermal diffusivities shown in Table I using the relationship $\kappa = D\gamma T_{e0}$. Figure 7 shows the dependence of κ on initial electron temperature. The error bars in the plot indicate the standard deviations of the fitted values. When κ is assumed to depend on the temperature, its tendency can be explained by the relaxation time approximation (RTA). In a previous report,[19] the temperature dependence of κ was expressed as

$$\kappa = \frac{1}{3} v_F^2 \frac{\gamma T_e}{AT_e^2 + BT_l} \tag{4}$$

by deviating from $1/\tau = AT_e^2 + BT_l$ and a general expression of $\kappa = (1/3)v_F^2 \tau \gamma T_e$, where v_F is the electron Fermi velocity, A and B are constants and τ is the electron relaxation time. Using the experimental value of the electron velocity $1.02 \times 10^6\,\mathrm{m{\cdot}s^{-1}}$ for v_F[5] and the temperature coefficient of the thermal resistivity,[23] A is calculated as $6.5 \times 10^6\,\mathrm{K^{-2}{\cdot}s^{-1}}$. Since κ is assumed to be $317\,\mathrm{W{\cdot}m^{-1}{\cdot}K^{-1}}$ at $T_e = 300\,\mathrm{K}$,[18] B is chosen as $6.9 \times 10^{10}\,\mathrm{K^{-1}{\cdot}s^{-1}}$. Theoretical values of κ are shown in Fig. 7. For the equilibrium state of $T_l = T_e$ in eq. (4), the calculated values of κ agree well with the values found in

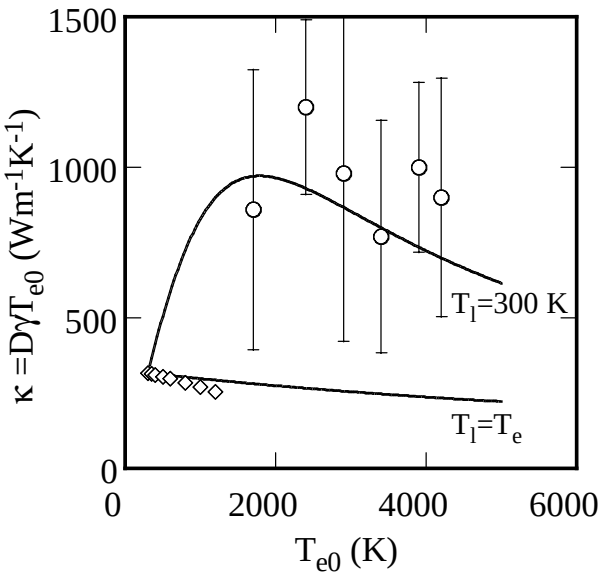

Fig. 7. Comparison between experimental and theoretical values of κ, where ○ and ◇ indicate experimental results for hot electrons and literature values for equilibrium state (ref. 18), respectively. Solid lines: theoretical predictions for equilibrium state ($T_l = T_e$) and nonequilibrium state ($T_l = 300$ K).

the literature (diamond[18]). The predictions for nonequilibrium states calculated by eq. (4) are shown in Fig. 7, where T_l is fixed at 300 K (ambient temperature) in eq. (4). Our results seem to be explained well by eq. (4) without adjustable parameters. However, there is some question as to whether or not the expression of the relaxation time in eq. (4) is valid. The calculation by eq. (4) predicts that κ has a maximum value at $T_e = 1700$ K, which means that the electronic resistivity of a metallic sample has a minimum value at a high temperature of 1700 K. The prediction that κ increases with rising T_e for $T_e < 1700$ K seems to require careful consideration.

On the other hand, when κ is assumed to be independent of the temperature, our results may not be explained by the RTA. In this case, one possibile explanation of our results is that hot electrons act as ballistic particles, even on a time scale of several picoseconds after thermalization. When the mean-free path of the electrons is assumed to be on the same order of the excitation fringe spacing Λ, the scattering time is estimated as several picoseconds. Although the ballistic behaviors of photoexcited electrons in metals before their thermalization have been reported,[5] ballistic behaviors of hot electrons after thermalization have not been pointed out, to our knowledge. This nonthermal property of the hot electrons on time scales of picoseconds may be similar to that in discussions of the electron-phonon coupling process.

5. Conclusions

The direct measurements of electron-phonon coupling and transport processes of hot electrons in the surface plane have been performed on a gold thin film. The possibility that fs-TRG measurements can be a powerful tool for studying ultrafast dynamics in metals was demonstrated. Our TRG measurements and analysis, based on TTM, showed that the electron-phonon coupling process and thermal diffusion can be investigated independently and quantitatively. From the discussion regarding the electron-phonon coupling factor G and the thermal conductivity κ, nonthermal processes on time scales of picoseconds were suggested. However, some interesting problems as to the hot electron properties, such as temperature dependences of G and κ, remain. These energy dissipation processes of hot electrons are expected to affect the surface displacement dynamics such as the generation of longitudinal acoustic waves and surface acoustic waves. The applicability of the TRG method in the investigation of the surface displacement dynamics has been demonstrated by our research.[12–15] The results of the surface displacement dynamics monitored by the fs-TRG will be discussed elsewhere. Since the photothermal methods, including the TGR method, have useful properties such as interface selectivity, dynamic investigations can be applied to more complicated systems. The fs-TRG method is also expected to be a powerful tool for investigating femtochemistry at solid/liquid interfaces.[24]

Acknowledgement

This work is supported by a Grant-in-Aid for Specially Promoted Research (No. 07102004) from the Ministry of Education, Science, Sports and Culture.

1) *Ultrafast Phenomena IV*, eds. D. H. Auston and K. B. Eisenthal (Springer-Verlag, Berlin, 1984) Chap. 2.
2) W. S. Fann, R. Storz, H. W. K. Tom and J. Bokor: Phys. Rev. Lett. **68** (1992) 2834.
3) N.-H. Ge, C. M. Wong, R. L. Lingle Jr., J. D. McNeill, K. J. Gaffney and C. B. Harris: Science **279** (1998) 202.
4) S. D. Brorson, J. G. Fujimoto and E. P. Ippen: Phys. Rev. Lett. **59** (1987) 1962.
5) C. Suárez, W. E. Bron and T. Juhasz: Phys. Rev. Lett. **75** (1995) 4536.
6) C.-K. Sun, F. Vallée, L. Acioli, E. P. Ippen and J. G. Fujimoto: Phys. Rev. B **48** (1993) 12365.
7) S. I. Anisimov, B. L. Kapeliovich and T. L. Perel'man: Sov. Phys. JETP **39** (1975) 375.
8) A. P. Kanavin, I. V. Smetanin, V. A. Isakov, Yu. V. Afanasiev, B. N. Chichkov, B. Wellegehausen, S. Nolte, C. Momma and A. Tunnermann: Phys. Rev. B **57** (1998) 14698.
9) B. Huttner and G. C. Rhor: Appl. Surf. Sci. **126** (1998) 126.
10) I. M. Fishman, C. D. Marshall, J. S. Meth and M. D. Fayer: J. Opt. Soc. Am. B **8** (1991) 1880.
11) C. M. Li, T. Sjodin and H. L. Dai: Phys. Rev. B **56** (1997) 15252.
12) T. Tanaka, A. Harata and T. Sawada: Jpn. J. Appl. Phys. **35** (1996) 3642.
13) Q. Shen, A. Harata and T. Sawada: Jpn. J. Appl. Phys. **35** (1996) 2339.
14) A. Harata, N. Adachi and T. Sawada: Phys. Rev. B **58** (1998) 7319.
15) K. Katayama, T. Sawada, Q. Shen and A. Harata: Phys. Rev. B **58** (1998) 8428.
16) T. Juhasz, H. E. Elsayed-Ali, G. O. Smith, C. Suárez and W. E. Bron: Phys. Rev. B **48** (1993) 15488.
17) H. J. Eichler, P. Gunter and D. W. Pohl: *Laser-Induced Dynamic Grating* (Springer-Verlag, Berlin, 1986).
18) *CRC Handbook of Chemistry and Physics*, ed. D. R. Lide (CRC Press, Boca Raton, 1993) 74th ed.
19) X. Y. Wang, D. M. Riffe, Y.-S. Lee and M. C. Downer: Phys. Rev. B **50** (1994) 8016.
20) H. E. Elsayed-Ali and T. Juhasz: Phys. Rev. B **47** (1993) 13599.
21) P. B. Allen: Phys. Rev. Lett. **59** (1987) 1460.
22) J. P. Girardeau-Montaut and C. Girardeau-Montaut: Phys. Rev. B **51** (1995) 13560.
23) A. H. MacDonald: Phys. Rev. Lett. **44** (1980) 489.
24) A. Hibara, A. Harata and T. Sawada: Chem. Phys. Lett. **272** (1997) 1.